Punctiform initiation of seafloor spreading in the Red Sea during transition from a continental to an oceanic rift

Enrico Bonatti

Lamont-Doherty Geological Observatory, Columbia University, Palisades, New York 10964, USA

Transition from a continental to an oceanic rift occurs in the Red Sea by initial emplacement of oceanic crust in regularly spaced 'hot points', which serve as nuclei for axial propagation into segments of oceanic crust accretion and for initiation of seafloor spreading. Hot points develop above upwelling mantle diapirs caused by density/viscosity inversion beneath continental and oceanic rifts.

AN important goal in earth science is to understand how the transition from a continental to an oceanic rift occurs in time and space, which will further our knowledge of oceanic Atlantic-type passive margins. This transition, which occurred along the proto-Atlantic rift 160–90 Myr ago, can be observed today in the northern Red Sea. Based on morphotectonic, magnetometric, seismic-reflection and petrological data from this region, I will attempt to demonstrate that: (1) injection of oceanic crust takes place initially in punctiform hot areas axially spaced ~50 km apart; (2) activation of hot points shows a northward time progression; and (3) each hot point serves as a nucleus for axial propagation of the zone of oceanic crust accretion into linear segments of spreading. I will also explain the punctiform initiation of seafloor spreading in terms of inferred patterns of upper mantle upwelling beneath the Red Sea, and suggest that the same model can be applied to the initial opening of the Atlantic rift.

Plate-tectonic reconstructions of the Red Sea/Gulf of Aden region[1–5] suggest that, although emplacement of oceanic crust between Arabia and Africa initiated in the Gulf of Aden as early as ~10 Myr ago[6], it started more recently in the Red Sea[7]. An axial rift valley with strong magnetic signature is present almost continuously in the southern Red Sea between 16° and 19° N. Vine–Matthews-type axial magnetic anomalies indicate initiation of seafloor spreading by injection of basalt crust in a narrow axial zone ~5 Myr BP in a region around 17° N, but more recently to the north and south of this region[8], in a pattern which suggests axial rift propagation[9]. Moving northward, the axial rift valley and associated magnetic signature become discontinuous and then disappear completely in the northern Red Sea (Figs 1, 2).

This description assumes that, outside the axial zone with clear-cut high-amplitude Vine–Matthews magnetic anomalies, the Red Sea is floored by thinned, stretched continental crust criss-crossed by diffuse basaltic dyke injections, a view supported by recent geophysical data collected at sea[7,10–12] and by observations at Zabargad (St John) Island, an uplifted block of Red Sea lithosphere[13]. However, the concept that the whole width of the Red Sea formed by two stages of seafloor spreading, the first of which started as early as ≈40 Myr BP, has also been proposed[14,15].

The axial zone of the Red Sea can be divided from south to north into the following regions (Fig. 1), based on their different morphotectonic and magnetometric characteristics[7,8,12,16–18]: (1) rift valley region (17° N–19°30′ N), with a relatively straight and continuous axial rift valley and linear magnetic anomalies; (2) multi-deeps region (19°30′ N–22° N), with a complex pattern of axial deeps and troughs; (3) transitional region (22° N–24° N), with a few regularly spaced axial trough segments; (4) northern region (north of 24° N), with no axial rift valleys but a few isolated deeps. The model proposed here is based primarily on results obtained from the transitional region.

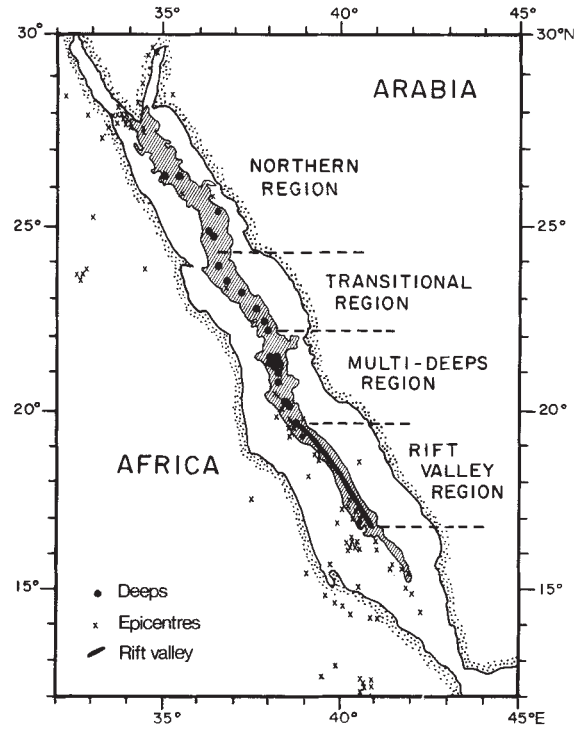

Fig. 1 Outline of the Red Sea, with the axial zone enclosed by the 500-fathoms isobath. The approximate location of the axial rift valley and of isolated deeps and troughs is indicated. Also shown are locations of earthquake epicentres of magnitude >4 recorded from 1953 to 1983. The axial zone has been subdivided into geotectonic regions (see text).

Red Sea transitional region

Field work in this region (Fig. 2) has shown the existence of segments of axial troughs and deeps with high-amplitude magnetic anomalies, separated by intertrough zones which lack an axial rift valley and high-amplitude magnetic anomalies, and have continuous, thick sediment cover across the axis[11,16–18].

The transitional region axial trough segments, named (from south to north) Thetis, Nereus, Bannock and Vema[11,16], become shorter, narrower and shallower moving from south to north (Fig. 2*a*, *b*). The Thetis and Nereus segments display morphotectonic features typical of rift valleys of oceanic slow-spreading axial zones such as the Mid-Atlantic Ridge (MAR). They have

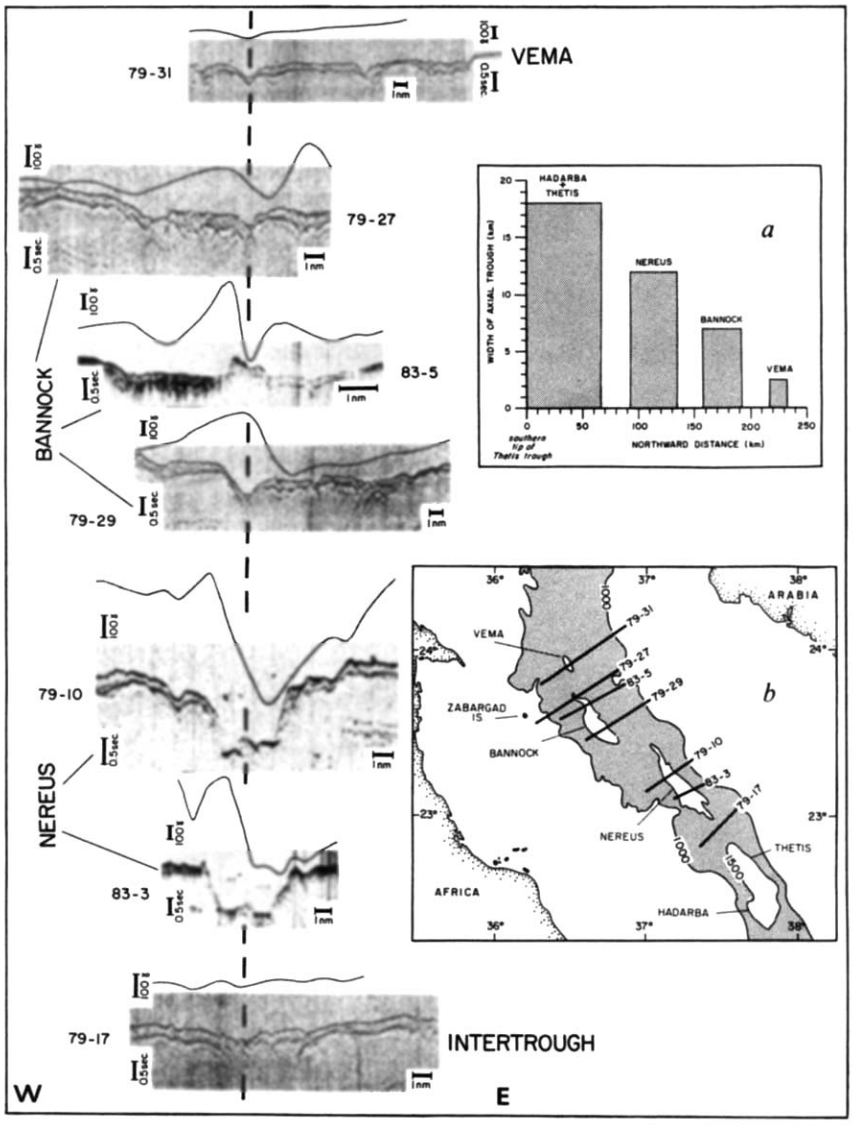

Fig. 2 Outline of the Red Sea transitional region where the axial troughs and deeps (Thetis–Hadarba, Nereus, Bannock and Vema) are shown enclosed by the 1,500-m isobath (insert *a*). A series of seismic reflection profiles taken across the Red Sea axis (locations indicated in insert *b*) is shown on the left of the figure, together with magnetic anomalies along the same profiles. The vertical broken line indicates the approximate axis of the Red Sea. Insert *b* shows the width and length of the Thetis–Hadarba, Nereus, Bannock and Vema axial trough and deeps, defined by the 1,500-m isobath. Length is estimated from the distance along the Red Sea axis taken from the southern end of the Thetis–Hadarba trough.

steep walls formed by inward-facing normal faults[18] and a neovolcanic zone floored by young basalts with mid-ocean ridge basalt (MORB) affinity[11]. A trough segment to the south of Thetis, termed Hadarba Deep[16], merges with Thetis although the axes of the two segments are offset laterally by ~5 km (Fig. 2*b*). High-amplitude magnetic anomalies are present at Thetis[15], although its scant coverage does not allow an accurate estimate of the time of initiation of seafloor spreading. Its wider, longer and deeper trough suggests that Thetis is older and more evolved than Nereus. Magnetic anomalies over the Nereus trough suggest the presence of oceanic crust and initiation of seafloor spreading ~1 Myr ago in sections across the northern and southern parts of the trough, but >2 Myr ago in sections from the central part of the trough[11]. Thus, the Nereus axial trough could be considered a mini-propagating oceanic rift segment where oceanic crust was emplaced initially in a central spot which then served as a nucleus for axial propagation.

The next axial deep segment to the north of Nereus, the Bannock Deep, lacks a steep axial rift valley but shows a gentle graben-like morphology with continuous sediment cover except along one section where a 500-m-high basement protrudes from the sediment (Fig. 2, profile 83-5). This feature is probably a volcanic seamount because fragments of dolerite were recovered from it[11]. Profiles taken across the axis a few kilometres north and south of the seamount indicate continuous sediment cover and a prominent fault aligned axially with the volcanic seamount (Fig. 2). Narrow high-amplitude magnetic anomalies are associated with the seamount and the axial fault.

The Vema axial deep consists of a relatively gentle depression with continuous sediment cover and no high-amplitude magnetic anomalies, but there is relatively high heat flow[11]. A consistent pattern of axial high-amplitude magnetic anomalies is absent in the Red Sea north of the Vema Deep, although deeps and anomalies have been found at several isolated sites[16,18,19].

Punctiform initiation of seafloor spreading

The observations from the Red Sea transitional region lead to the following interpretations, summarized in part in Fig. 3:

(1) The initial breakthrough of oceanic crust and the beginning of organized seafloor spreading occurs in essentially punctiform hot areas located in axially oriented segments of tensional fissures. The initial breakthrough of oceanic crust would occur through continental crust which has been thinned, stretched and diffusely injected by basaltic dykes[7,10,11], although it could occur in ancient, cold oceanic crust if the two-stage opening model[14,15] is accepted. The igneous body cropping out from the axis of the Bannock graben and the axial fault detected just south and north of this igneous body are examples of recent hot point formation.

(2) Axial propagation from each hot point gives rise to linear spreading segments[9]. This hypothesis is supported by the detection of magnetic anomalies, as old as 2–3 Myr in sections from the centre of the Nereus trough segment, but younger close to the tips of the segment.

(3) A northward progression can be detected in the time of initial activation of the punctiform areas of ocean crust emplace-

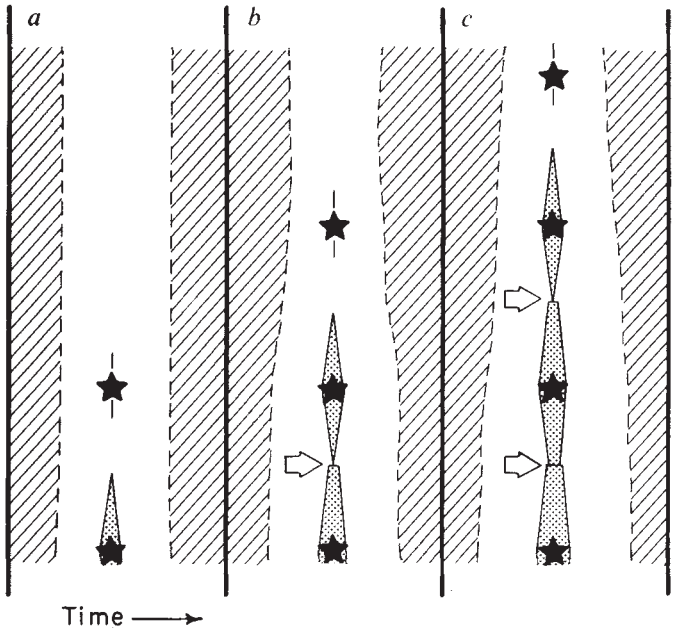

Fig. 3 Schematic model of the initiation of seafloor spreading in the Red Sea transitional region. *a–c*, Different stages in time. Stars indicate sites of hot points where the initial emplacement of oceanic crust occurs. Striped areas, continental; stippled areas, oceanic; open areas, intermediate continental crust stretched, thinned and injected by basaltic dykes. Arrows, discontinuities in the morphotectonic and magnetic axial pattern, predicted by the model.

ments. Although in the southern Red Sea (between 17° N and 18° N), seafloor spreading initiated ~5 Myr BP, emplacement of oceanic crust probably started between 2 and 3 Myr BP at Nereus; it started <1 Myr BP at Bannock and has not yet started at Vema. The observation that the Thetis trough is deeper and wider than Nereus suggests that it is more evolved, and is therefore older than Nereus. Relatively high heat flow, as detected within the Vema Deep[11], may be a precursor to oceanic crust emplacement and may therefore mark future hot points in the northern Red Sea.

(4) The distance between the centre points of Thetis, Nereus, Bannock and Vema is ~50 km (Fig. 2*b*), suggesting a regular spacing of the areas of upper mantle upwelling and oceanic crust initial emplacement.

(5) Axial propagation from each hot point will eventually lead to joining of the different rift segments. Discontinuities are likely to develop in the axial morphotectonic and magnetic lineations where the tip of rift segments derived from different hot points join (Fig. 3). Moreover, the axial troughs and deeps are not all aligned; some show lateral offsets (Fig. 2). These initial offsets in the segments of oceanic crust emplacement may or may not lead to the formation of initial transform faults.

(6) The regular segmentation of the axis of spreading (Fig. 3) is interrupted where the Red Sea lithosphere is intersected by pre-existing shear zones[20], which would prevent normal axial rift popagation and act as 'locked zones' in the sense described by Courtillot[9].

I now consider how the proposed model, derived from observations in the transitional region, fits available data from other regions of the Red Sea.

Rift Valley region. The evolution of seafloor spreading from a punctiform initiation can be inferred from observations obtained in the southern Red Sea between 17° N and 19°30′ N (Fig. 1). The relatively continuous axial trough and the associated high-amplitude magnetic anomalies imply a steady though asymmetrical seafloor spreading regime for the past few million years, with spreading being about two-thirds faster to the west than to the east[8,16].

A detailed investigation of the axial zone at 18° N, including direct submersible observations[21,22], has revealed a morphotectonic structure of the axial trough similar to that of the MAR in the FAMOUS area, a neovolcanic zone with basalts similar to MORB, and a spreading rate averaging 1.6 cm yr^{-1} for the past 3–5 Myr. A deep-tow profile (Fig. 4) of the axial zone at 17°30′ N (ref. 23) confirmed a morphotectonic structure similar to that found in the FAMOUS area, and demonstrated asymmetrical spreading (≃5 mm yr^{-1} to the east, 10 mm yr^{-1} to the west) starting at 4.8 Myr BP. In the context of the proposed model it is of interest that the Rift Valley morphotectonic structures and high-amplitude magnetic anomalies run along the axis in this region for straight segments 30–50-km long, which are stepped laterally by small, 3–10-km transform or non-transform relay zones (Fig. 4) where the magnetic anomalies are weak and irregular[12]. One such discontinuity was surveyed in detail at 18° N (ref. 21). The proposed model explains these discontinuities as marking sites where different rift segments meet, each created by longitudinal propagation from an initial hot point (Fig. 3).

Multi-deeps region. This region, located between the more evolved southern Red Sea and the transitional region (Fig. 1), displays a complex geotectonic situation: the straight axial rift valley is replaced by a network of deeps distributed partly in an 'echelon' pattern[16–18,24]. Some of these deeps are thermally active at present and contain hot brines (for example, Atlantis II, Discovery); some are instead inactive[24]. This complex geotectonic structure may be determined in part by the presence of a major transverse fracture zone intersecting the Red Sea axis[17,20,25], an interpretation supported by the clustering of recent earthquake epicentres in this area (Fig. 1), and by the orientation of magnetic anomalies transversal to the Red Sea axis[17]. This is one of three major fracture zones intersecting the Red Sea, the other two being the Zabargad and the Brothers fracture zones, all striking parallel to the Dead Sea–Aqaba fault[20].

Northern region. The Red Sea north of the Vema Deep lacks a regular pattern of axial rift valley segments and associated high-amplitude magnetic anomalies[7,11], though a few isolated deeps are present, some located off the axis (Fig. 1). Some are associated with magnetic anomalies; that is, Charcot Deep at 25° N, where non-MORB basalts intrude the sediment[19], and Al Wajab Deep at 25°20′ N, where the anomalies are lineated partly in a direction transversal to the Red Sea axis[15,19]. Some of these deeps may represent small pull-apart basins caused by tectonics related to the fracture zone, such as Al Wajab, at the northeastern end of the Zabargad Fracture Zone, where the Red Sea axial direction shifts by ≃40° (Fig. 1).

Following Cochran[7], I interpret the northern Red Sea region as floored by thinned and stretched continental crust injected by diffuse basaltic intrusions. Probable examples of such intrusions are basaltic/gabbroic rocks from the Brothers Islets[26] and the Charcot Deep[19], showing transitional or alkaline affinity, in contrast to the MORB-like characteristics of basalts from the Nereus Trough[11] and from other axial sites further south in the Red Sea[27]. Thus, punctiform axial injection of oceanic crust and organized seafloor spreading have probably not yet started in the northern region of the Red Sea.

Mantle upwelling beneath the Red Sea

The punctiform model of initiation of seafloor spreading in the Red Sea implies that beneath each initial hot point there is a zone of preferential upwelling of upper mantle material. It is generally agreed that a broad thermal anomaly affects the upper mantle in major rift zones of the Earth. One of the tenets of plate-tectonic theory is that the asthenosphere/lithosphere boundary rises close to the surface along the axis of oceanic rifts[28]. A rise of the upper-mantle isotherms and of the asthenosphere/lithosphere boundary has been documented for major continental rifts, such as the East African[29], Rio Grande[30,31], Rhinegraben[32] and Baikal[33,34] rifts. A rise of upper-mantle isotherms and a thinning and stretching of the lithosphere, probably resulting in part from convective heat transfer to its base[35], obtains also beneath the Red Sea rift, a view consistent

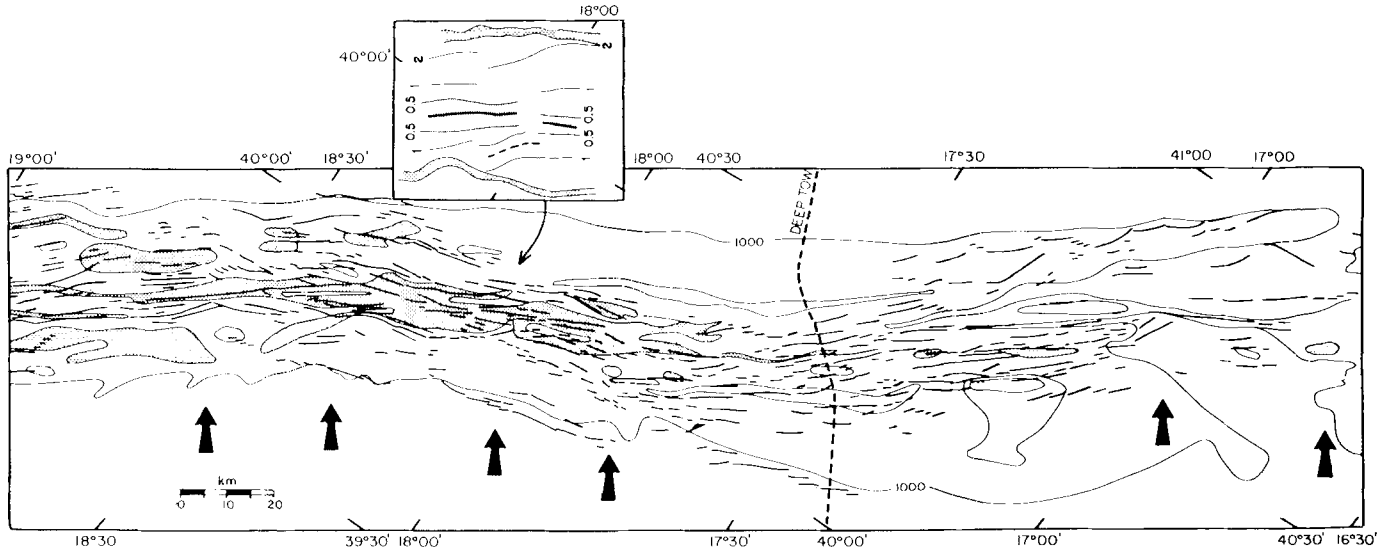

Fig. 4 A portion of the axial zone of the rift valley region of the Red Sea, with simplified bathymetry, from Backer *et al.*[16], and structural lineations obtained by a GLORIA sidescan survey, from Garfunkel *et al.*[12]. Arrows indicate discontinuities in the axial morphotectonic lineations observed by Garfunkel *et al.*[12]. Insert shows details of one such discontinuity at 18°, simplified from Zonenshajn *et al.*[21]. Isochrons (in Myr), based on magnetic anomalies, are indicated. Thick full line, present axis; dashed thick line, fossil axial segment; shadowed area, outer slopes of rift valley.

with a broad band of high heat flow[36] and positive gravity anomaly[37] extending across the entire width of the Red Sea.

Continuous upwelling and decompression of upper-mantle material below rift zones leads to partial melting. A low-density/viscosity layer containing a continuously replenished small melt fraction would result, sandwiched between material of higher density and viscosity. The low density of this layer is enhanced by the probability that the upwelling mantle is injected by metasomatic, H_2O- and CO_2-rich fluids, resulting in H_2O-containing phases, such as amphiboles. This mantle metasomatism is important below continental rifts[38].

The presence beneath the Red Sea of an upper mantle zone containing a melt fraction and affected by metasomatism is suggested by studies of a mantle-derived spinel lherzolite body uplifted on Zabargad Island (Fig. 2*b*), probably during the early stages of Red Sea rifting[13,39]. The lherzolite body contains zones of plagioclase peridotite, probably representing small fractions of melt trapped by lherzolites in the upper mantle, as well as amphibole peridotites produced by reactions of metasomatic fluids with the lherzolite[40].

The density/viscosity inversion in the upper mantle can be treated as a Raleigh–Taylor-type instability, an approach which has been used to model the distribution of volcanic activity along island arcs[41] and oceanic spreading zones[42,43]. Theory and experiments[41,44–47] indicate that the interface between a high density/viscosity upper layer and a layer below with lower density/viscosity develops a sinusoidal instability that may evolve into a pattern of λ-spaced injections of the lower density fluid into the denser layer above. The density contrast affects the velocity of upwelling of the diapirs according to Stoke's law. Their spacing, λ, is related to the ratio of the thicknesses of the upper and lower layer, h_1/h_2, and the ratios of their viscosities, μ_1/μ_2 (refs 45–47).

In the case of the Red Sea rift, the low-density upper mantle zone can be assumed to be elongated in shape and of limited width. Provided $h_1 > h_2$, the spacing of the diapirs surging from the lower layer is approximated by [41,45,46]:

$$\lambda = \frac{2\pi h_2}{2.15}(\mu_1/\mu_2)^{1/3}$$

Assuming μ_1 to be of the order of 10^{20} P[48,49], μ_2 can be estimated as being lower by 2–4 orders of magnitude, depending on the degree of partial melting chosen for h_2 and on the temperature and pressure contrast of the two layers. The thickness of h_2 depends on the upper mantle thermal regime of the particular rift being considered. Assuming h_2 as the layer containing melt within the 5–10% range, its thickness beneath the Red Sea axis should be a few kilometres, as estimated from data from Iceland[50] and mid-ocean ridges[43,48]. If $\mu_1/\mu_2 = 10^3$ and $h_2 = 2$ km are chosen, a spacing slightly over 50 km is obtained for the upwelling diapirs.

Upwelling of the diapirs would result in an increased degree of melting, with the melt tending to segregate from its parent, collect towards the top of the diapirs and hence be injected into the crust. The attenuated thickness of the Red Sea crust would permit the 'asthenosphere geoid'[51,52] and hence the melt to reach the sea floor. This mantle-driven pattern leading to the punctiform geometry of initial breakthrough of oceanic crust (Fig. 5), however, is interrupted where the Red Sea lithosphere is intersected and disrupted by pre-existing fracture zones, as in the multi-deeps region and in the Zabargad Fracture Zone.

The northward time progression in the activation of the hot points and in the evolution of seafloor spreading in the Red Sea suggests that the asthenospheric diapirs are superimposed on a broader zone of shallow hot upper mantle which may be moving as a wavefront towards the northern Red Sea (Fig. 5).

Axial propagation from each initial hot point could take place by mechanisms similar to the asthenospheric longitudinal flow

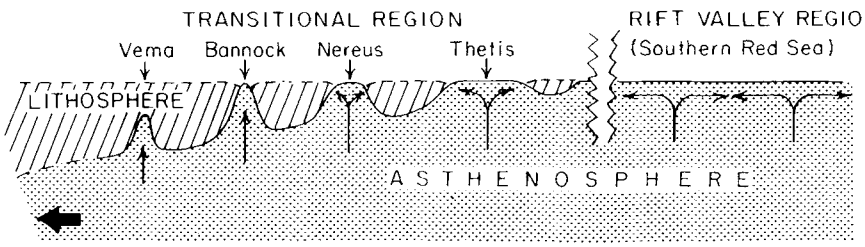

Fig. 5 Schematic and hypothetical cross-section along the axis of the Red Sea, showing regularly spaced asthenospheric diapirs in the transitional region, possibly caused by Raleigh–Taylor instability in the upper mantle, superimposed on a broad wavefront of shallow hot mantle moving northward beneath the Red Sea.

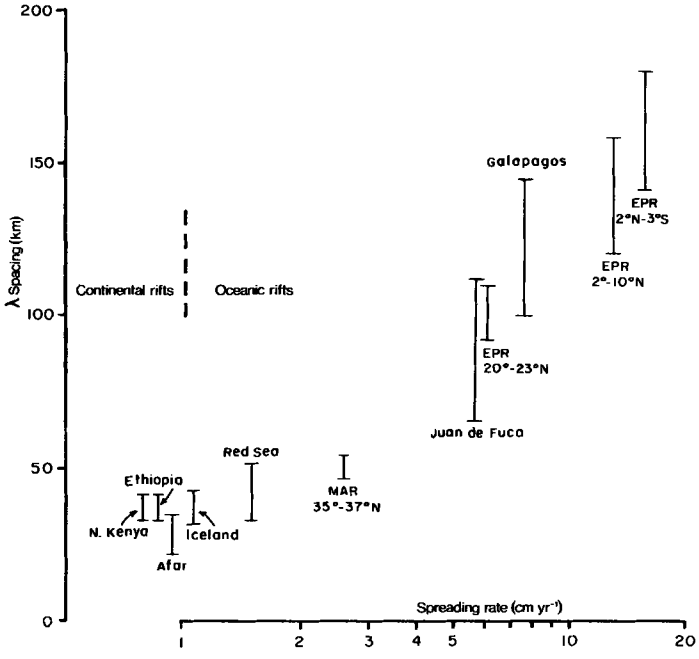

Fig. 6 Spacing of axial volcanism in continental, proto-oceanic and oceanic rifts, versus spreading rate for the oceanic rifts. Data for the East Pacific Rise (EPR), MAR, Galapagos rift and Juan De Fuca Ridge are from Crane[43]. Data for the Red Sea are from the present paper; for Iceland they include Quaternary and Recent volcanism of the East Volcanic Zone, from Sigurdsson and Sparks[56]; for North Kenya, Ethiopian and Afar rifts they include Quaternary and Recent volcanism, from Mohr and Wood[57].

described by Courtillot[9] and Vogt[53], and would result in axial spreading segments similar to those 30–50-km long observed in the rift valley region of the southern Red Sea. Interestingly, Mesozoic (155–108 Myr BP) magnetic anomalies from the western North Atlantic reveal that close to the time of opening, the early Atlantic accretionary axis was divided in segments each ~50 km long with discontinuities of the magnetic anomalies, not necessarily associated with transform offsets, between each segment[54]. Therefore, it seems that the punctiform model of initiation of seafloor spreading proposed for the Red Sea can also be applied to the early Atlantic rift.

Evolution from continental to oceanic rift

Structural studies of peridotites from ophiolite complexes suggest vertical flow of upper-mantle material beneath oceanic ridges, with upwelling zones spaced 50–100 km apart[55]. Crane[43] noted that the spacing between areas of upwelling and igneous activity in oceanic zones of crustal accretion is related to spreading rate, that is, ≈150 km along the fast East Pacific Rise, ≈100 km along the intermediate Galapagos rift and Juan de Fuca Ridge, and ≈50 km along the slow MAR. A regular spacing of ~40 km has been noted for active volcanoes in the eastern volcanic zone of Iceland, part of the MAR[56]. The concept of regularly spaced volcanism can be extended to continental rifts: a spacing of ≈40 km has been reported for Pleistocene and active volcanoes of the northern Kenya and Ethiopian rifts, and of 30–10 km for those of the Afar rift[57]. The increase in spacing of hot points from continental to proto-oceanic, to slow, intermediate and fast oceanic rifts (Fig. 6) is paralleled by an inferred uplift of sub-rift isotherms and asthenosphere/lithosphere boundary, an increase in the degree of upper-mantle melting and a change in melt chemistry from alkaline to transitional to tholeiitic and to MORB. The first factor above, causing an increase in the thickness of the zone of partial melting from continental to slow to fast-spreading rifts[43,48], would determine a corresponding increase in the spacing of asthenospheric diapirs and volcanism. Thus, the transition from continental to oceanic rift as seen in the central Red Sea could be considered an important step in a continuum of rift processes, related ultimately to the evolution of mantle thermal waves.

The field work which led to this paper was sponsored by the Italian Research Council (CNR). I thank the officers and crew of RV *Bannock*; D. Breger, P. Colantoni, K. Crane and M. Taviani for collaboration; and J. Cochran for help in modelling the magnetic anomalies. The research was supported by NSF grant O.C.E. 83-15933 and by ONR contract N00014-8-C-0098. Contribution no. 3833 of the Lamont-Doherty Geological Observatory.

Received 5 December 1984; accepted 5 May 1985.

1. McKenzie, D. P. *Earth planet. Sci. Lett.* **40**, 25–32 (1978).
2. Freund, R. *Nature* **228**, 453–455 (1970).
3. Girdler, R. W. & Darracot, B. W. *Geophysics* **2**, 131–138 (1972).
4. Richardson, E. S. & Harrison, C. G. A. *Earth planet. Sci. Lett.* **30**, 135–142 (1976).
5. LePichon, X. & Francheteau, J. *Tectonophysics* **46**, 369–406 (1978).
6. Cochran, J. R. *Geophys. J. R. astr. Soc.*, **68**, 171 (1982).
7. Cochran, J. R. *Bull. Am. Ass. Petrol. Geol.* **67**, 41–69 (1983).
8. Roeser, H. A. *Geol. Jb.* **13**, 131–153 (1975).
9. Courtillot, V. E. *Tectonics* **1**, 239–250 (1982).
10. Coleman, R. G. *Proc. 27th Int. geol. Congr., Moscow S-06-2-1* **23**, 93–121 (1984).
11. Bonatti, E., Colantoni, P., Della Vedova, B. & Taviani, M. *Oceanologica acta* **7**, 385–398 (1984).
12. Garfunkel, Z., Ginzburg, A. & Searle, R. C. *Anns Geophyisica* (in the press)
13. Bonatti, E. *et al. J. geol. Soc.* **140**, 677–690 (1983).
14. Girdler, R. W. & Styles, P. *Nature* **247**, 7–11 (1974).
15. Hall, S. A. *Saudi Arabian Proj. Rep. 275* (US Geol. Surv. 1979).
16. Backer, H., Lange, K. & Richter, H. *Geol. Jb.* D13, 79–123 (1975).
17. Searle, R. C. & Ross, D. A. *Geophys. J. R. astr. Soc.* **43**, 555–572 (1975).
18. Pautot, G. *Oceanologica Acta* **6**, 235–244 (1983).
19. Pautot, G., Guennoc, P., Coutelle, A. & Lyberis, N. *Nature* **310**, 133–136 (1984).
20. Crane, K. & Bonatti, E. *Tectonophysics* (submitted).
21. Zonenshajn, L. P., Monin, A. S. & Sorokhtin, G. *Geotektonika* **2**, 3–22 (1981).
22. Juteau, T. *et al. Bull. Centres. Rech. Explor. Prod. Elf-Aquitaine* **7**, 217–231 (1983).
23. Miller, S. P., MacDonald, K. C. & Lonsdale, P. F. *J. geophys. Res.* (in the press).
24. Degens, E. T. & Ross, D. A. (eds) *Hot Brines and Recent Heavy Metal Deposits in the Red Sea* (Springer, Berlin, 1969).
25. Garson, M. S. & Krs, M. *Bull. geol. Soc. Am.* **87**, 169–181 (1976).
26. Taviani, M., Bonatti, E., Colantoni, P. & Rossi, P. L. *Boll. geol. Soc. Ital.* (in the press).
27. Schilling, J. G. *Science* **165**, 1357–1360 (1969).
28. Sclater, J. G. & Francheteau, J. *Geophys. J. R. astr. Soc.* **20**, 509–542 (1970).
29. Baker, B. H. & Wohlenberg, J. *Nature* **229**, 538–542 (1971).
30. Bridwell, R. J. in *Tectonics and Geophysics of Continenta. Rifts* (eds Ramberg, H. & Neumann, E. R.) 73–80 (Reidel, Boston, 1978).
31. Parker, E. C., Davis, P. M., Evans, J. R., Iyer, H. M. & Olsen, K. H. *Nature* **312**, 354–356 (1984).
32. Edel, J. B., Fuchs, K., Gelbke, C. & Prodehl, C. *J. geophys. Res.* **41**, 333–345 (1975).
33. Logatchev, N. A., Rogozhina, V. A., Solonenko, V. P. & Zorin, Y. A. in *Tectonics and Geophysics of Continental Rifts* (eds Ramberg, I. B. & Neumann, E. R.) 49–62 (Reidel, Boston, 1978).
34. Zorin, Y. A. *Tectonophysics* **73**, 91–104 (1981).
35. Spohn, T. & Schubert, G. *J. geophys. Res.* **87**, 4669–4681 (1982).
36. Girdler, R. W. & Evans, T. R. *Geophys. J. R. astr. Soc.* **51**, 245–251 (1977).
37. Allan, T. D. *Phil. Trans. R. Soc.* **A267**, 153–180 (1970).
38. Bailey, D. K. *Nature* **296**, 525–530 (1982).
39. Bonatti, E., Ottonello, G. & Hamlyn, P. R. *Geology* **9**, 474–479 (1981).
40. Bonatti, E., Ottonello, G. & Hamlyn, P. R. *J. geophys. Res.* (in the press).
41. Marsh, B. D. *J. Geol.* **87**, 687–713 1979).
42. Whitehead, J. A., Dick, H. J. B. & Shouten, H. *Nature* **312**, 146–148 (1984).
43. Crane, K. *Earth planet. Sci. Lett.* **72**, 405–414 (1985).
44. Danes, Z. F. *Geophysics* **29**, 414–424 (1964).
45. Biot, M. A. & Ode, H. *Geophysics* **30**, 213–227 (1965).
46. Seelig, F. *Geophysics* **30**, 633–634 (1965).
47. Ramberg, H. *Phys. Earth planet. Inter.* **5**, 45–60 (1972).
48. Lewis, B. T. R. *J. geophys. Res.* **86**, 4868–4880 (1981).
49. Rabinowicz, M., Nicolas, A. & Vigneresse, J. L. *Earth planet. Sci. Lett.* **67**, 97–108 (1984).
50. Thayer, R. E., Bjornsson, A., Alvarez, L. & Hermance, J. F. *Geophys. J. R. astr. Soc.* **65**, 423–442 (1981).
51. Turcotte, D. L., Haxby, W. F. & Ockendon, J. R. in *Island Arcs, Deep Sea Trenches and Back-Arc Basins* (eds Talwani, M. & Pitman, W. C.) 63–69 (Am. Geophys. Union, 1977).
52. LePichon, X. & Sibuet, J. C. *J. geophys. Res.* **86**, 3708–3720 (1981).
53. Vogt, P. R. *Earth planet. Sci. Lett.* **29**, 309–325 (1976).
54. Shouten, H. & Klitgord, K. D. *Earth planet. Sci. Lett.* **59**, 255–266 (1982)
55. Nicolas, A. & Violette, J. F. *Tectonophysics* **81**, 319–339 (1982).
56. Sigurdsson, H. & Sparks, S. R. *Nature* **274**, 126–130 (1978).
57. Mohr, P. A. & Wood, C. A. *Earth planet. Sci. Lett.* **33**, 126–144 (1976).